© 2015. Published by The Company of Biologists Ltd | Development (2015) 142, 2941-2950 doi:10.1242/dev.120774

RESEARCH ARTICLE

STEM CELLS AND REGENERATION

Root developmental programs shape the *Medicago truncatula* nodule meristem

Henk J. Franssen[1,‡], Ting Ting Xiao[1], Olga Kulikova[1], Xi Wan[1,*], Ton Bisseling[1,2], Ben Scheres[3] and Renze Heidstra[3]

ABSTRACT

Nodules on the roots of legume plants host nitrogen-fixing *Rhizobium* bacteria. Several lines of evidence indicate that nodules are evolutionarily related to roots. We determined whether developmental control of the *Medicago truncatula* nodule meristem bears resemblance to that in root meristems through analyses of root meristem-expressed *PLETHORA* genes. In nodules, *MtPLETHORA 1* and *2* are preferentially expressed in cells positioned at the periphery of the meristem abutting nodule vascular bundles. Their expression overlaps with an auxin response maximum and *MtWOX5*, which is a marker for the root quiescent center. Strikingly, the cells in the central part of the nodule meristem have a high level of cytokinin and display *MtPLETHORA 3* and *4* gene expression. Nodule-specific knockdown of *MtPLETHORA* genes results in a reduced number of nodules and/or in nodules in which meristem activity has ceased. Our nodule gene expression map indicates that the nodule meristem is composed of two distinct domains in which different *MtPLETHORA* gene subsets are expressed. Our mutant studies show that *MtPLETHORA* genes function redundantly in nodule meristem maintenance. This indicates that *Rhizobium* has recruited root developmental programs for nodule formation.

KEY WORDS: *Medicago truncatula*, Nodule meristem, *PLETHORA* genes, *DR5*

INTRODUCTION

The interaction between legumes and soil-borne bacteria, collectively known as rhizobia, leads to the formation of new organs called root nodules (Stougaard, 2001; Limpens and Bisseling, 2003). As nodules are formed on roots it has been hypothesized that the nodule developmental program is derived from the lateral root developmental program (Nutman, 1948; Hirsch et al., 1997; Mathesius et al., 2000; de Billy et al., 2001; Roudier et al., 2003; Bright et al., 2005; Desbrosses and Stougaard, 2011). Recently, the expression of several root meristem regulators has been observed in the nodule meristem (NM) (Osipova et al., 2011, 2012; Roux et al., 2014), thereby providing molecular support for this hypothesis. However, whether the identified genes function in the formation of NM and root meristem (RM), a prerequisite for concluding that the nodule developmental program is derived from that of the root, has thus far remained unclear.

Root tissues are continuously replenished by stem cells, and in *Arabidopsis* these stem cells surround the quiescent center (QC) cells (Dolan et al., 1993). The QC functions as a so-called organizer and is essential for maintenance of the surrounding stem cells (van den Berg et al., 1997), and together they form the stem cell niche. The daughter cells of these stem cells form files of transit-amplifying cells and, together with the stem cell niche, they form the RM (Heidstra and Sabatini, 2014). Auxin accumulation is crucial for the specification of the stem cell niche in the *Arabidopsis* RM, which colocalizes with an auxin concentration and response maximum (Sabatini et al., 1999; Blilou et al., 2005; Petersson et al., 2009). Several *Arabidopsis* transcription factors have been identified that are required for proper formation and function of the root stem cell niche, among them WUSCHEL-RELATED HOMEOBOX 5 (WOX5) (Sarkar et al., 2007), SCARECROW (SCR) (Di Laurenzio et al., 1996; Sabatini et al., 2003) and four PLETHORA (PLT) factors (Aida et al., 2004; Galinha et al., 2007). *WOX5* transcript accumulates specifically in the QC and mutant analyses have revealed that it is required for columella stem cell maintenance (Sarkar et al., 2007). *PLT* genes are part of the small *AINTEGUMENTA-LIKE* (*AIL*) gene clade of transcriptional regulators within the large *AP2/ERF* family (Horstman et al., 2014). Among this clade, *PLT1-4* are essential for root formation as their higher order mutants are rootless (Galinha et al., 2007). In *plt1, plt2* double mutants, stem cells and transit-amplifying cells are lost, while ectopic *PLT1* and *PLT2* expression is sufficient to induce root niche formation (Aida et al., 2004; Galinha et al., 2007). This shows that a combination of PLT1 and PLT2 is most indicative for RM activity. A gradient of PLT activity controls root zonation and the highest PLT concentration localizes to the stem cell niche (Mähönen et al., 2014).

Legume nodule formation is initiated by dedifferentiation of cortical cells, which divide and form the nodule primordium. Upon infection by the microsymbiont, the NM is formed at the apex of the primordium (Timmers et al., 1999; Stougaard, 2001; Limpens and Bisseling, 2003). In the model legume *Medicago*, which forms nodules with a persistent meristem at its apex, nodule development can be divided into six stages based on the sequential pattern of anti- and periclinal cell divisions in inner cortical cell layers C3-C5, endodermis and pericycle (Xiao et al., 2014). The cluster of cells formed up until stage V is called the nodule primordium. It consists of six to eight cell layers derived from pericycle and endodermis, about eight cell layers of infected cells derived from the inner cortical cell layers C5 and C4, and a few cell layers derived from cortical cell layer C3 that will develop into the NM (Xiao et al., 2014). From stage VI onward the *Medicago* nodule apical meristem becomes functional and adds cells to different nodule tissues: the central tissue, consisting of infected and non-infected cells,

[1]Department of Plant Sciences, Laboratory of Molecular Biology, Wageningen University, Droevendaalsesteeg 1, Wageningen 6708 PB, The Netherlands. [2]College of Science, King Saud University, Post Office Box 2455, Riyadh 11451, Saudi Arabia. [3]Department of Plant Sciences, Plant Developmental Biology, Wageningen University, Droevendaalsesteeg 1, Wageningen 6708 PB, The Netherlands.
*Present address: NOVOGENE Bioinformatics Technology, 38 Xueqing Road, Haidian District, Beijing, China.

[‡]Author for correspondence (henk.franssen@wur.nl)

Received 5 December 2014; Accepted 24 July 2015

Development (2015) 142, 2941-2950 doi:10.1242/dev.120774

and the peripheral tissues including the nodule cortex, endodermis and parenchyma. The latter contains vascular bundles that develop from nodule vascular meristems (NVMs) (Roux et al., 2014). The part of the NM that adds cells to the central tissue forms a large domain at the apex and is composed of four to six cell layers. Transition of meristem cells to the central tissue cells is accompanied by a switch from mitosis to endoreduplication in the cells that become infected by rhizobia (Cebolla et al., 1999).

Recent studies confirmed the expression of orthologs of a number of known *Arabidopsis* RM regulators in the nodule, among them *MtWOX5*, *MtPLT2* and *MtBBM/PLT4* (Osipova et al., 2011, 2012; Roux et al., 2014). These genes appeared to be expressed in the central meristem region and at the tip of the nodule vascular bundles, where maximum DR5 activity is also observed (Couzigou et al., 2014), suggesting that a root-like developmental program is operational in the NM. To functionally address whether the nodule developmental program is regulated by factors similar to those that are key in controlling the *Arabidopsis* root developmental program, we studied the expression of *MtPLT* genes in the NM and the effect of their knockdown on nodule formation. Based on these results we propose that the NM consists of distinct central and peripheral meristematic domains and that four *MtPLT* genes (*MtPLT1-4*) redundantly control nodule formation and NM maintenance. This is reminiscent of the described function of *AtPLT* genes in root development and suggests that rhizobia have recruited major regulators of root development.

RESULTS

Medicago truncatula orthologs of *AtPLT* genes

Recent studies showed that orthologs of *AtPLT* genes, named *MtPLT2(Medtr4g65370)* and *MtBBM/PLT4(Medtr7g080460)* are expressed in the NM (Boutilier et al., 2002; Hofhuis et al., 2013; Limpens et al., 2013; Roux et al., 2014). We asked whether the other *Medicago PLT* orthologs are also expressed in the NM and performed reciprocal BLAST searches (in Mt4.0v1) using the AtPLT protein sequences as a query to identify their homologs in *Medicago* (Table 1; supplementary material Fig. S1) (Tamura et al., 2011). Alignment of all *Arabidopsis* and *Medicago* PLT protein sequences using *Vitus vinifera* as an outgroup shows that there are single *Medicago* orthologs of *AtBBM/PLT4* and *AtPLT5*, which we named *MtPLT4(Medtr7g080460)* and *MtPLT5(Medtr4g127930)*, respectively (supplementary material Fig. S1). The phylogeny of the AtPLT1/2 and AtPLT3/7 subclades indicates that in *Medicago* ancestral gene duplications have occurred, independent from those observed in *Arabidopsis*, generating *Medtr2g09180* and *Medtr4g65370* that reside in the *AtPLT1/2* clade and *Medtr5g031880* and *Medtr8g068510* that reside in the *AtPLT3/7* clade. Because of the independent gene duplication events in *Arabidopsis* and *Medicago* a direct orthology link between genes in the *PLT1/2* and *PLT3/7* clades cannot be drawn. Nevertheless, comparison of the expression patterns indicates that *AtPLT3* and *Medtr5g031880* are expressed in the RM, whereas *AtPLT7* and *Medtr8g068510* are not [Galinha et al., 2007; Prasad et al., 2011; The *Medicago truncatula* Gene Expression Atlas Project (http://mtgea.noble.org/v3/)]. Based on these data and to keep in line with the previously designated *MtPLT2* (Limpens et al., 2013), we utilize from now on the following nomenclature: *Medtr2g098180* (*MtPLT1*), *Medtr4g065370* (*MtPLT2*), *Medtr5g031880* (*MtPLT3*) and *Medtr7g080460* (*MtPLT4*) (Table 1). The proposed gene annotations were subsequently used to design primers (supplementary material Table S5) to enable gene expression studies by qPCR. Our data reveal that all four *MtPLT* genes are expressed in nodules, albeit at lower levels than in roots (Fig. 1A).

Table 1. Accession numbers of *A. thaliana* and *M. truncatula* *PLETHORA* genes

Gene	*A. thaliana*	*M. truncatula*
PLT1	*At3g20840*	*Medtr2g098180*
PLT2	*At1g51190*	*Medtr4g065370*
PLT3	*At5g10510*	*Medtr5g031880*
PLT4 (*BBM*)	*At5g17430*	*Medtr7g080460*

The annotation for *Medicago PLT1* and *PLT2* is arbitrary (but following a previous annotation by Limpens et al., 2013) because *Medicago* and *Arabidopsis PLT1* and *PLT2* genes were formed by independent gene duplication events (see supplementary material Fig. S1). *Medtr5g031880* resides together with *Medtr8g068510* in the *PLT3*/7 clade. Because *Medtr5g031880* is, like *AtPLT3*, expressed in the RM whereas *Medtr8g068510* is not, we annotated *Medtr5g031880* as *PLT3*.

A pre-existing and growing root that can be inoculated to induce nodulation is crucial for the analysis of *MtPLT* function in nodules. Therefore, the maintenance of the RM, a process for which four redundantly acting *PLT* genes are essential in *Arabidopsis* (Aida et al., 2004; Galinha et al., 2007; Mähönen et al., 2014), should be ensured. To this end, the function of *MtPLT* genes must be tested in the *Medicago* RM. At present, mutants are only available for *MtPLT 1*, *2* and *4* (http://bioinfo4.noble.org/mutant/), hampering the generation of a quadruple mutant in *Medicago* as a tool to determine via genetics whether the four *MtPLT* genes are the redundantly acting orthologs of *Arabidopsis PLT1-4*. Instead, we reduced the expression of *MtPLT1* and *MtPLT2* (*MtPLT1i,2i*), or of *MtPLT3* and *MtPLT4* (*MtPLT3i,4i*) or of all four *MtPLT* genes (*MtPLTi*) simultaneously by RNA interference (RNAi) under the control of the *35S* promoter by *Agrobacterium rhizogenes*-mediated root transformation (supplementary material Fig. S2) (Limpens et al., 2004). Eight days after transferring the transformed plantlets to perlite, we counted the number of roots growing from transgenic calli. On 18 calli of empty vector-transformed plantlets, 58 transgenic roots of more than 3 cm in length were grown (supplementary material Fig. S2A-C, arrow; Table S1). By contrast, no transgenic roots longer than 3 cm were grown from 16 calli of *35SMtPLTi* plants. On these calli, only four transgenic roots of 1-2 cm in length were grown (supplementary material Fig. S2H,I, arrowhead) and numerous small outgrowths were detected (supplementary material Fig. S2E,F, red). Analyses of the transgenic short roots shows that the RM is absent, indicating the rapid differentiation of meristematic cells (supplementary material Fig. S2G-I). On 20 calli of *35SMtPLT1i,2i* transgenic plants 13 short and 9 long transgenic roots were grown, while on 27 calluses of *35SMtPLT3i,4i* plants 12 short and 66 long transgenic roots were grown (supplementary material Table S1). Thus, downregulation of *MtPLT1* and *MtPLT2* has a more profound effect on RM maintenance than downregulation of *MtPLT3* and *MtPLT4*. This shows that, in analogy to *Arabidopsis* (Aida et al., 2004; Galinha et al., 2007; Mähönen et al., 2014), *MtPLT1-4* redundantly act on root formation and growth and that downregulation of all four *MtPLT* genes severely affects root formation.

MtPLT genes are required for nodule development and NM maintenance

We next asked whether downregulation of individual *MtPLT* genes influences nodule growth, as it was possible that individual members have specific functions in nodules despite the redundancy in their roles in root development. We reduced the expression of the individual *MtPLT* genes by RNAi under the control of the *35S*

Development (2015) 142, 2941-2950 doi:10.1242/dev.120774

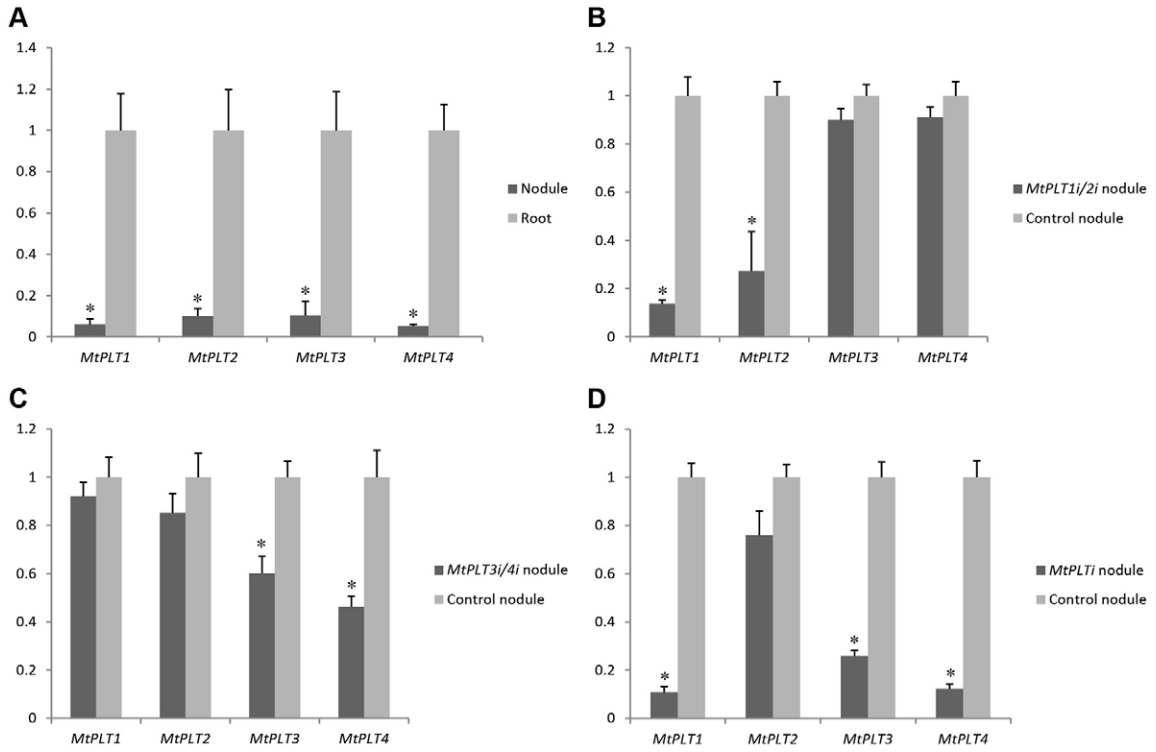

Fig. 1. Quantification of *MtPLT* expression levels in non-transgenic roots and nodules and RNAi nodules. (A) Relative *MtPLT* expression is lower in 15-day-old nodules than in roots (expression is normalized to 1 in roots for each *MtPLT* gene). (B-D) Relative *MtPLT* expression in 15-day-old transgenic nodules of *ENOD12::MtPLT1i,2i* (B), *ENOD12::MtPLT3i,4i* (C) and *ENOD12::MtPLTi* (D) with respect to expression in control nodules (normalized to 1 for each *MtPLT* gene). Quantification was normalized using *MtACTIN-2* as reference gene. Shown are the mean±s.e.m. of two (A) or three (B-D) biological replicates. The value of each biological replicate is based on technical triplicates. **P*<0.05 (Student's *t*-test).

promoter by *A. rhizogenes*-mediated root transformation. We analyzed nodules formed on at least 15 transgenic roots 15 days post inoculation in experimental duplicates. The level of *MtPLT* gene expression reduction was determined by qPCR on RNA isolated from roots and nodules (supplementary material Fig. S3A-E). This showed that different degrees of RNA reduction were obtained for the different genes in roots as well as in nodules. Notably, RNAi was specific for each of the targeted *MtPLT* genes (supplementary material Fig. S3A-D). However, RNAi did not lead to a significant reduction in nodule number compared with the number of nodules formed on control roots in all replicates (supplementary material Table S2). Next, we investigated in detail the effect of single *MtPLT* gene knockdown on nodule development by analysis of serial microsections of control and transgenic nodules by counting the cell layers in the meristem, infection zone and the fixation zone. Analyses of 20 control nodules collected per replica shows that the NM consists of 4-6 cell layers and the central tissue of 16-19 cell layers distributed over 6-7 cell layers in the infection zone and 10-12 cell layers in the fixation zone (Fig. 2A). We did not observe significant differences between the number of cell layers in single *MtPLT* knockdown and control nodules (supplementary material Fig. S4, Table S3). Altogether, these results indicate that downregulation of individual *MtPLT* genes had no significant effect on nodule development. Subtle effects, however, might have gone unseen owing to variation between transgenic roots after a hairy root transformation (Limpens et al., 2004).

Downregulation of *MtPLT1* and *MtPLT2* has a more profound effect on RM maintenance than downregulation of *MtPLT3* and *MtPLT4*. To demonstrate the effect of reducing gene expression of more than one *MtPLT* gene in nodules, we conducted RNAi using the *MtENOD12* promoter. During nodule ontogenesis this gene is activated in the nodule primordium, the NM and in the infection zone of mature nodules (Limpens et al., 2009, 2013). We tested the effect of *ENOD12::MtPLT1i,2i*, *ENOD12::MtPLT3i,4i* and *ENOD12::MtPLTi* in triplicate on nodule growth and development. Importantly, *ENOD12::MtPLTi* did not affect transgenic root growth from calluses upon *A. rhizogenes*-mediated transformation (supplementary material Table S1).

The level of downregulation of the *MtPLT* genes was determined by qPCR (Fig. 1B-D). We confirmed that *MtPLT1* and *MtPLT2* RNA levels were reduced in transgenic *ENOD12::MtPLT1i,2i* nodules, whereas *MtPLT3* and *MtPLT4* RNA levels were not (Fig. 1B). Similarly, *MtPLT3* and *MtPLT4* RNA levels were reduced in *ENOD12::MtPLT3i,4i* nodules, whereas *MtPLT1* and *MtPLT2* RNA levels were not (Fig. 1C). In transgenic *ENOD12::MtPLTi* nodules, all four *MtPLT* genes were reduced in expression, albeit to different levels (Fig. 1D). On transgenic *ENOD12::MtPLTi*, *ENOD12::MtPLT1i,2i* or *ENOD12::MtPLT3i,4i* roots the number of nodules was significantly reduced (Mann-Whitney test, $P<0.01$ for *ENOD12::MtPLTi*, $P<0.05$ for *ENOD12::MtPLT1i,2i* and *ENOD12::MtPLT3i,4i*; supplementary material Table S4) compared with control roots.

All compound *ENOD12::MtPLT* RNAi transgenic nodules were smaller than those on control transgenic roots. To determine potential causes of the size reduction, we analyzed longitudinal sections of transgenic nodules collected in triplicate 15 days after inoculation, and observed a high percentage of phenotypically aberrant nodules (Fig. 2, Table 2). We classified the nodule phenotypes into two groups: class I, in which the number of cell layers in meristem and infection zone is reduced (Fig. 2B,D); and

Development (2015) 142, 2941-2950 doi:10.1242/dev.120774

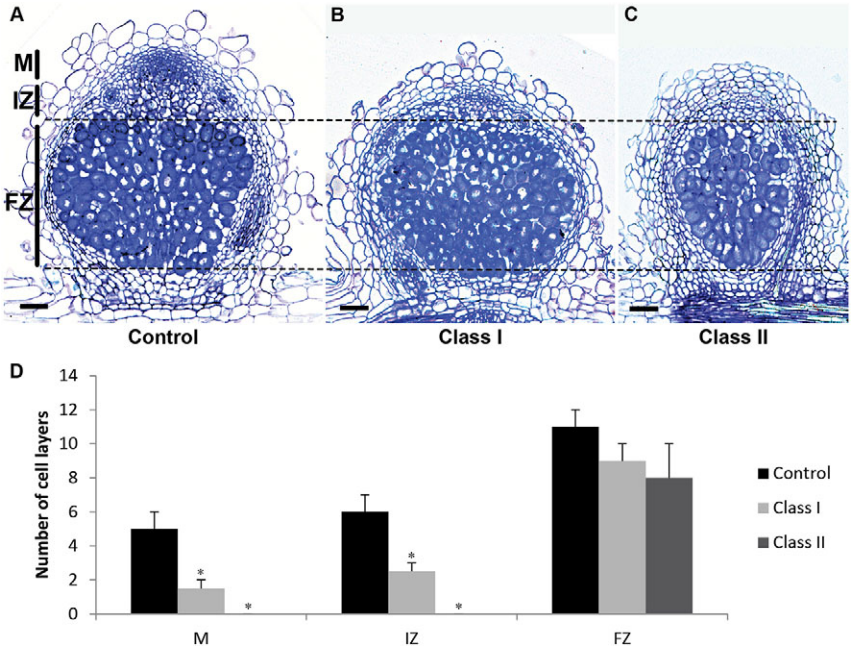

Fig. 2. RNAi of *MtPLT* genes affects *Medicago* nodule development. (A) Control wild-type nodule. In addition to nodules of wild-type appearance, two classes of nodules are formed when more than one *MtPLT* gene is knocked down. (B) Representative class I nodule. The number of cell layers in meristem (M) and infection zone (IZ) is reduced. (C) Typical class II nodules lacking a meristem and infection zone. All infected cells in the fixation zone (FZ) originate from primordium cells derived from C4 and C5 cortex layers. (D) Comparison of the average number of cell layers in meristem, infection zone and fixation zone in 20 control and 16 *ENOD12::MtPLTi* (5 class I and 11 class II) show that the meristem and infection zone are not present in class II nodules, whereas in class I nodules the number of meristem and infection zone cell layers is reduced. **P*<0.05 (Student's *t*-test). Error bars indicate s.e.m. Scale bars: 75 µm.

class II, which lack the NM and the infection zone (Fig. 2C,D). These class II nodules only consist of six to ten layers of infected cells (Fig. 2C). Notably, a complete block of meristem formation still permits the generation of nodules with six layers of infected cells, which are derived from the C4 and C5 cortical cells (Xiao et al., 2014). These results indicate that *MtPLT* activity is needed for proper NM formation and maintenance, but not for the infection of primordium cells. This does not exclude the possibility that *MtPLT* gene activity may be required for the infection of cell layers in the infection zone derived from the NM.

In nodules formed on *ENOD12::MtPLT1i,2i* and *ENOD12::MtPLT3i,4i* roots, the majority of the affected nodules were grouped into class I (Table 2). By contrast, the majority of *ENOD12::MtPLTi* nodules fell into class II (*n*=11 out of 16, Table 2). These results show that the downregulation of all four *MtPLT* genes simultaneously has a more dramatic effect on NM formation and maintenance than the downregulation of a combination of only two *MtPLT* genes. In conclusion, our results show that *MtPLT* genes redundantly affect NM formation.

MtPLT promoter activity marks the *Medicago* RM

A striking difference between *PLT*-directed root and nodule growth is that *MtPLT3i/4i* affects nodule growth, whereas *Atplt3/Atplt4* knockout and *MtPLT3i/4i* knockdown minimally affect root growth (Fig. 2, Table 2; supplementary material Table S1) (Galinha et al., 2007). To seek an explanation for this discrepancy, we compared the expression patterns of the different *MtPLT* genes using *pMtPLT::GUS* fusions in root and nodule and *in situ* hybridization (ISH) in nodule. *MtPLT* mRNA localization in nodules is in agreement with the GUS staining pattern observed from the respective promoter fusion, indicating that the *pMtPLT::GUS* fusions reflect the true expression pattern of the corresponding genes (Roux et al., 2014) (compare supplementary material Fig. S5 with Fig. 6). In *Arabidopsis*, *AtPLT3* and *AtBBM*/*PLT4* are expressed in the RM in a pattern that overlaps with, but is slightly different from, that of *AtPLT1* and *AtPLT2* (Galinha et al., 2007). Before testing the activity of *MtPLT* promoters in the NM, we first identified their activity pattern in the root and compared these to markers for auxin (*DR5*) and cytokinin (*TCS*) response and QC activity (*WOX5*).

In primary *Medicago* roots, cell files converge to a group of cells that are suggested to be QC cells (Fig. 3A, arrow). Distal to the presumptive QC cells are the columella cells that accumulate starch granules (Fig. 3A). Similar to the pattern observed in *Arabidopsis* (Sabatini et al., 1999), in *Medicago* roots the highest level of expression from an integrated *DR5::GUS* construct is detected in the proposed stem cell niche (Fig. 3B). Comparison of *MtPLT1::GUS*, *MtPLT2::GUS*, *MtPLT3::GUS* and *MtPLT4::GUS* expression patterns shows that they overlap most in the RM. The highest expression domains coincide with the root stem cell niche, similar to *AtPLT* gene expression patterns (Galinha et al., 2007). However, the *MtPLT3::GUS* (Fig. 3E) and *MtPLT4::GUS* (Fig. 3F) expression patterns extend into the vascular tissue (supplementary material Fig. S6). It is interesting that AtPLT3 and AtBBM/PLT4

Table 2. Phenotypes of *MtPLT* RNAi nodules

RNAi	*n*	WT (%)	Class I (%)	Class II (%)	Class I+II (%)
ENOD12::MtPLT1i,2i	54	19 (35)	25 (46)	10 (19)	35 (65)
ENOD12::MtPLT3i,4i	23	9 (39)	9 (39)	5 (22)	14 (61)
ENOD12::MtPLTi	21	5 (24)	5 (24)	11 (52)	16 (76)
Control	50	47 (94)	3 (6)	0 (0)	3 (6)

n is the total number of nodules collected over three independent biological replicates. Class I: reduced number of layers of C3-derived meristem cells and of C4- and C5-derived infection zone. Class II: no meristem and no infection zone, only infected primordium cells derived from C4 and C5. Class I+II is the combined number of nodules with a phenotype. Phenotypes are statistically significantly different between *ENOD12::MtPLT1i,2i* or *ENOD12::MtPLT3i,4i* versus *ENOD12::MtPLTi* (*P*<0.05, Fisher's exact test). WT, wild type.

Development (2015) 142, 2941-2950 doi:10.1242/dev.120774

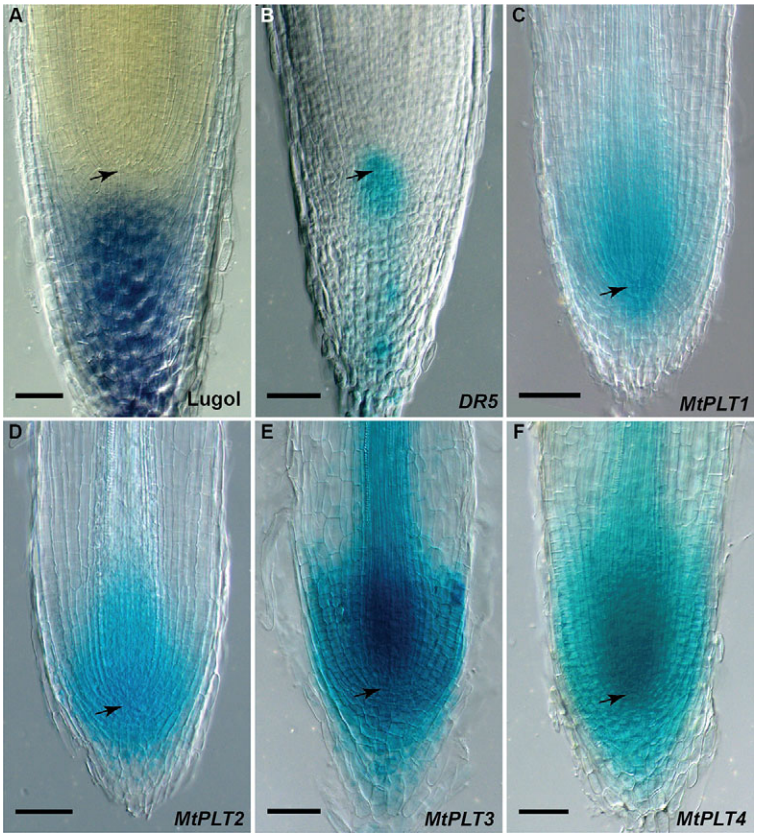

Fig. 3. *MtPLT* and *DR5* promoter activity in the *Medicago* root meristem. (A) *M. truncatula* root tip stained with lugol to visualize starch granules. Cell files converge to a central point showing the presence of presumptive QC cells. Distally are the columella cells that accumulate starch. (B) A *DR5::GUS* transgenic root shows *DR5* promoter activity in a cluster of cells encompassing the QC. (C-F) The *MtPLT1::GUS* (C), *MtPLT2::GUS* (D), *MtPLT3::GUS* (E) and *MtPLT4::GUS* (F) expression patterns overlap, with the highest activity in and around the QC. Arrows indicate the location of the presumptive QC. Scale bars: 75 µm.

fusion protein accumulation extends into the vascular tissue of the *Arabidopsis* root as well (Galinha et al., 2007). It has been shown that the activity pattern of *MtWOX5::GUS* also marks the proposed stem cell niche (Osipova et al., 2012). Hence, *MtPLT::GUS*, *DR5::GUS* and *MtWOX5::GUS* expression patterns can be used to mark RM-like compartments in *Medicago* nodule organogenesis.

MtPLT::GUS promoter activity in nodule primordia

The dramatic reduction in nodule numbers on the *MtPLTi* root indicates that *MtPLT* gene activity is crucial for nodule primordium formation. If so, *MtPLT* genes should be expressed in nodule primordia. To test this, we analyzed sections of *pMtPLT::GUS*-containing transgenic hairy roots for promoter activation in stage II-V nodule primordia (Fig. 4) (Xiao et al., 2014). Stage II-III nodule primordia (Fig. 4A,C,E,G) are characterized by active cell division in the pericycle and the innermost cortical cell layer, whereas endodermis cells are yet to divide (Xiao et al., 2014), and are distinct from *Medicago* lateral root primordia in which endodermis cell division precedes inner cortical cell division (Herrbach et al., 2014). The promoters of all four *MtPLT* genes are active in cells of stage II-III nodule primordia (Fig. 4A,C,E,G) and remain active in the later stages of nodule primordium development (Fig. 4B,D,F,H). These analyses revealed that the promoters of *MtPLT1-4* are indeed activated in nodule primordia (Fig. 4), corroborating their crucial role in nodule formation.

Patterns of *MtPLT* activation and the auxin and cytokinin response mark distinct domains in the NM

Cells in the *Medicago* NM divide for a prolonged time, suggesting that stem cells might contribute to the maintenance of the NM. *DR5::GFP* (Couzigou et al., 2014) and *MtWOX5::GUS* (Osipova et al., 2012) activity patterns have been allocated to distinct peripheral regions in the NM abutting vascular bundles (Fig. 5A,B, arrows). Assuming that *DR5::GUS* and *MtWOX5::GUS* colocalize to areas of stem cell activity in nodules, in analogy to the situation in roots, this suggests that stem cells are present in the NM periphery. Recently, the expression of several auxin-responsive genes in the central part of the NM has been reported (Limpens et al., 2013; Breakspear et al., 2015; Roux et al., 2014), suggesting that auxin signaling occurs in this region of the NM. Indeed, upon prolonged incubation (16 h), *DR5* activity becomes detectable throughout the vascular bundles and the nodule apex (Fig. 5C, arrowhead), including the central part of the NM. Such dynamics of GUS staining is only observed in *DR5::GUS* nodules and suggests that auxin signaling occurs throughout the NM, albeit at different levels in the central and peripheral parts.

For both *MtPLT1::GUS* and *MtPLT2::GUS*, we observed GUS activity foci in discrete domains within the nodule apex (Fig. 5D,E, arrows). These domains of high *MtPLT1* and *MtPLT2* promoter activity appear embedded in a region with lower GUS activation encompassing the NM. By contrast, *MtPLT3::GUS* and *MtPLT4::GUS* are activated throughout the nodule apex (Fig. 5F,G, arrowhead).

To determine whether the expression patterns of *DR5::GUS*, *MtWOX5::GUS*, *MtPLT1::GUS* and *MtPLT2::GUS* in the NM periphery overlap, we analyzed serial sections from the nodule apex downwards. *DR5* and *MtWOX5* activity is present in a subpopulation of cells within the apex adjacent to the vascular bundle (Fig. 6A,D). In subsequent sections, the radial tissue organization of a vascular bundle becomes apparent and all cells of this vascular bundle display *DR5* and *MtWOX5* activity (Fig. 6B,E). Finally, within this radially organized domain, xylem (Fig. 6, white arrow) and phloem can be discriminated. At the developmental stage corresponding to this position, the activity of

Development (2015) 142, 2941-2950 doi:10.1242/dev.120774

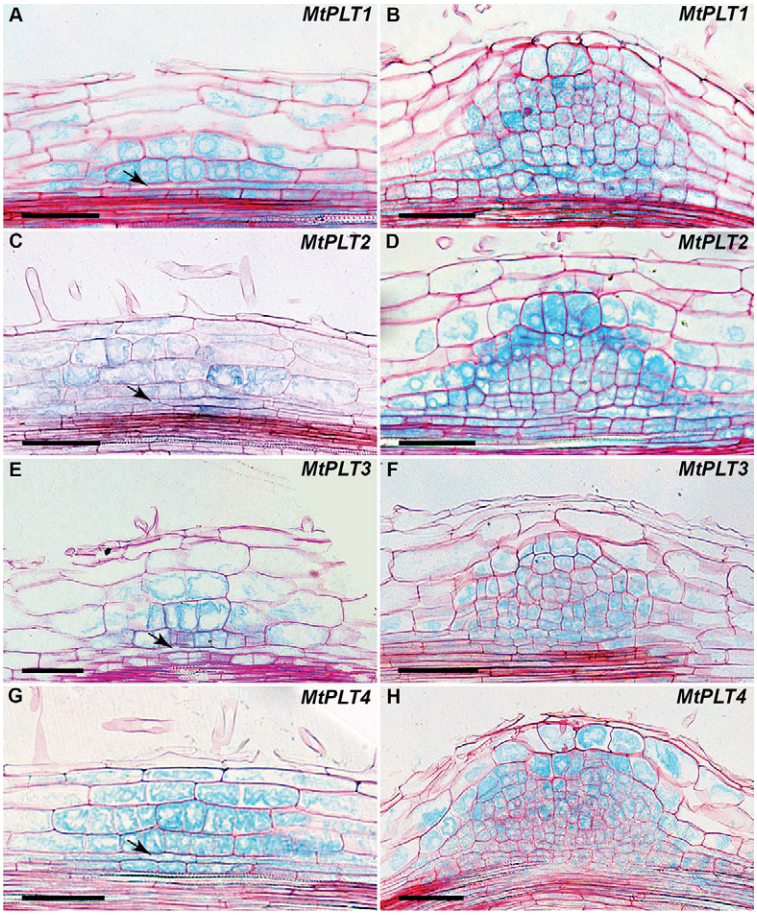

Fig. 4. *MtPLT* genes are activated in the nodule primordium. (A,C,E,G) Nodule primordia at stage II (according to Xiao et al., 2014) showing *MtPLT1::GUS* (A), *MtPLT2::GUS* (C), *MtPLT3::GUS* (E) and *MtPLT4::GUS* (G) activity. Endodermis (arrow) cells have not yet divided, whereas cortex cells have. (B,D,F,H) Nodule primordia of stage III-V showing expression of *MtPLT1::GUS* (B, stage IV), *MtPLT2::GUS* (D, stage III), *MtPLT3::GUS* (F, stage III) and *MtPLT4::GUS* (H, stage V) activity. Scale bars: 75 µm.

both *DR5* and *MtWOX5* decreases (Fig. 6C,F). Serial sections through *MtPLT2::GUS* nodules reveals that the highest GUS activity is restricted to cells that are contiguous with nodule vascular bundles (Fig. 6G-I, arrow), resembling the *DR5* (Fig. 6A-C) and the *MtWOX5* (Fig. 6D-F) promoter activity pattern. *MtPLT1::GUS* also displays its highest activity in NVM cells (Fig. 6J, arrow). These analyses show that *MtPLT1*, *MtPLT2*, *MtWOX5* and *DR5* are active in provascular tissue and cells abutting the provasculature, in analogy with their expression pattern in *Medicago* roots (Fig. 3B,D) (Osipova et al., 2011, 2012). A lower *MtPLT1::GUS* and *MtPLT2::GUS* activity is observed in cells in the central part of the NM (Fig. 6G-J, arrowhead). By contrast, representative sections of *MtPLT3::GUS* and *MtPLT4::GUS* stained nodules show that both mark the entire NM and, in addition, are also activated in cells of the infection zone (Fig. 6K,L), albeit at lower levels.

The colocalization of *MtPLT* gene expression and high *DR5* activity in the periphery of the NM suggests that an auxin-driven root-derived developmental program is operational in the nodule. In addition, several genes in the cytokinin signaling cascade are reported to be activated in the NM (Frugier et al., 2008; Plet et al., 2011; Mortier et al., 2014). To determine the cytokinin response distribution in the NM we studied the expression of *TCS::GUS*, a synthetic cytokinin-responsive promoter (Müller and Sheen, 2008), in transgenic *Medicago* roots and nodules. In roots, *TCS::GUS* activity encompasses mainly the QC and root cap and fades in the vasculature (Fig. 7A), which is similar to the activity in *Arabidopsis* roots (Zürcher et al., 2013). In contrast to the *DR5::GUS* activity

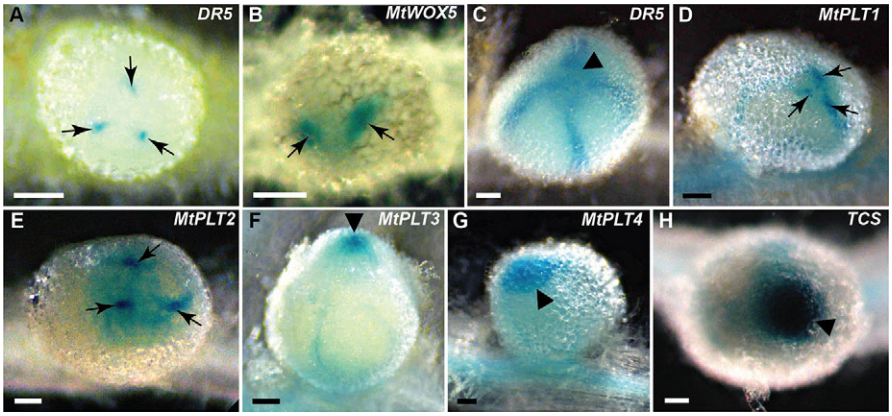

Fig. 5. *DR5*, *MtWOX5*, *MtPLT* and *TCS* promoter activities in nodules. (A,B) Top view of a *DR5::GUS* nodule (A) and an *MtWOX5::GUS* (B) nodule shows GUS activity in distinct regions at the periphery of the NM (arrows). (C) Upon prolonged incubation, GUS activity becomes apparent throughout the NM in *DR5::GUS* nodules (arrowhead). (D,E) Top views of *MtPLT1::GUS* (D) and *MtPLT2::GUS* (E) nodules show highest GUS activity in discrete regions in the periphery of the NM (arrows), with lower GUS activity throughout the NM. (F,G) *MtPLT3::GUS* (F) and *MtPLT4::GUS* (G) activity throughout the NM (arrowheads). (H) Top view of a *TCS::GUS* nodule marking the whole NM. All nodules were sampled 15 days after inoculation. Scale bars: 75 µm.

Development (2015) 142, 2941-2950 doi:10.1242/dev.120774

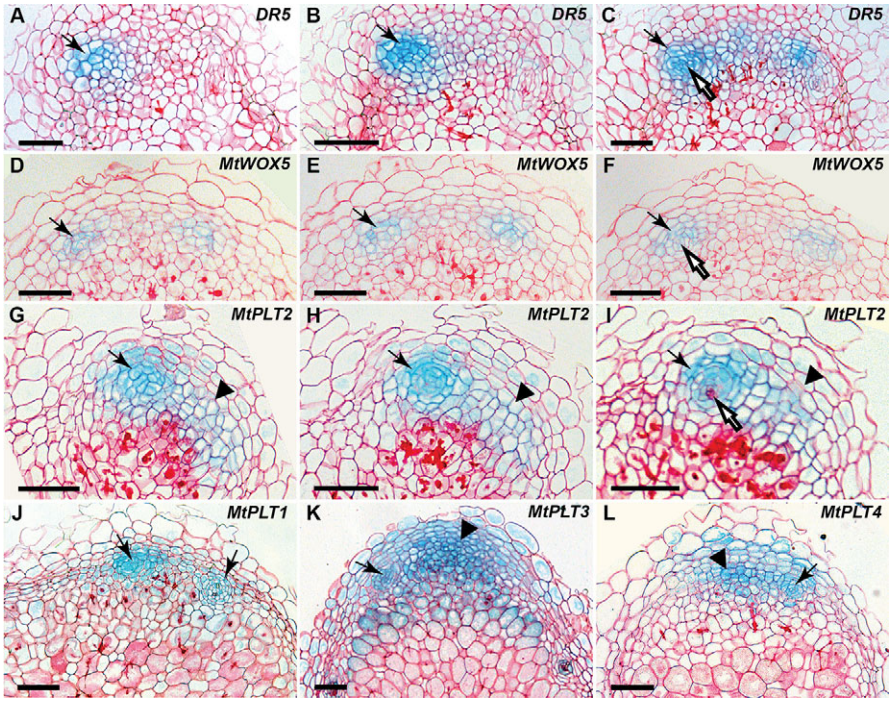

Fig. 6. *DR5::GUS*, *MtWOX5::GUS* and *MtPLT::GUS* expression patterns in nodules. (A-C) Serial tangential sections of 2 h-stained nodules to specifically localize the *DR5::GUS* activation region. *DR5* activity first appears in a group of cells (A, black arrow) that appear morphologically distinct from surrounding cells in the NM. In subsequent sections, *DR5* activity reached a maximum (B) and remains in cells that are part of the nodule vascular bundle (C). (D-F) Serial tangential sections of *MtWOX5::GUS* nodules shows a comparable pattern to *DR5::GUS*. White arrows indicate differentiation of xylem in the nodule vascular bundle (compare A and D, B and E, and C and F). (G-I) Serial sections of *MtPLT2::GUS* nodules show that the highest *MtPLT2::GUS* activity is in the NVM (black arrows). A lower *MtPLT2::GUS* activity is present in the central region of the NM (arrowheads). (J-L) Representative and illustrative serial sections showing that *MtPLT1::GUS* expression is also highest in the NVM (J, arrows), whereas *MtPLT3::GUS* (K) and *MtPLT4::GUS* (L) expression patterns show equal activity in NVM (arrow) and the central part of the NM (arrowhead). Scale bars: 75 µm.

pattern (Fig. 5A,C), *TCS::GUS* activity is equally distributed over the apex of the nodules (Fig. 5H). Longitudinal sections of these nodules show that *TCS::GUS* activity is confined to cells in the central part of the NM (Fig. 7B).

DISCUSSION

Here, we analyzed the expression pattern of *Medicago* orthologs of *Arabidopsis PLT1*, *PLT2*, *PLT3* and *BBM/PLT4* during root growth and nodule formation and maintenance in *Medicago*. We examined the effect of their downregulation by RNAi and showed that they act redundantly in *Medicago* root formation, demonstrating their orthology with *AtPLT1-4*. Nodulation-specific downregulation of *MtPLT* genes hampers nodule formation and growth. This is reminiscent of the redundancy in *AtPLT* function in root formation and growth (Galinha et al., 2007). Therefore, we conclude that root developmental programs have been co-opted for nodulation. Interestingly, whereas root growth in *Arabidopsis* is minimally affected in *plt3,plt4* plants (Galinha et al., 2007), nodule growth is affected in *MtPLT3i,4i* nodules. To seek an explanation we analyzed *MtPLT* expression in *Medicago* RM and NM.

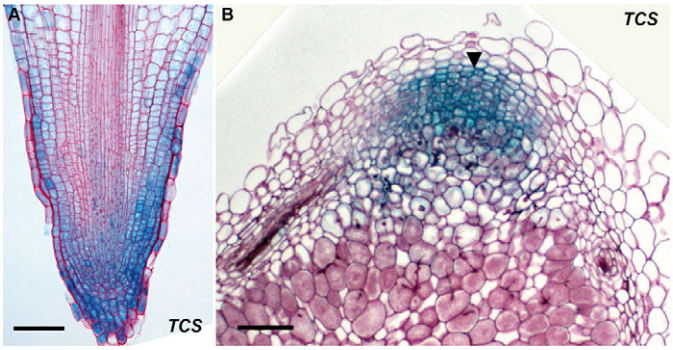

Fig. 7. *TCS::GUS* pattern in *Medicago* root and nodule. (A) *TCS::GUS* stained root shows activity in columella and lateral root cap cells. (B) In nodules, *TCS::GUS* activity is confined to the central region of the NM. Scale bars: 75 µm.

In *Arabidopsis* roots, the highest expression levels of *AtPLT1-4* colocalize in the stem cell niche (Galinha et al., 2007), which is also marked by *AtWOX5* (Sarkar et al., 2007) and *DR5* (Sabatini et al., 1999; Blilou et al., 2005; Petersson et al., 2009) activity. The root expression patterns of the *Medicago* and *Arabidopsis* orthologs are similar, with the exception of the extension of *MtPLT3* and *MtPLT4* expression higher up in the meristem and elongation zone. Therefore, the pattern of *pMtPLT3::GUS* and *pMtPLT4::GUS* in the root might point to a difference in the regulation of these genes between *Medicago* and *Arabidopsis*. In nodules *MtPLT1* and *MtPLT2* are highly expressed in regions located at the periphery of the NM, corresponding to the NVM. The highest auxin response activity and the activation of *MtWOX5::GUS* (Fig. 2B) (Osipova et al., 2012; Roux et al., 2014) coincide with the NVM. These expression patterns indicate that the developmental program directing peripheral tissue formation bears similarities to root developmental programs involving *PLT* genes (Galinha et al., 2007). However, in the absence of a suitable promoter that marks the NVM specifically, the effect of knockdown of *MtPLT* genes could not be tested in the NM periphery.

In addition to the high peripheral NM expression, *MtPLT1* and *MtPLT2* are expressed at lower levels in the central part of the NM, whereas *MtPLT3* and *MtPLT4* expression levels are comparable in both central and peripheral zones of the NM. In conclusion, based on the RM markers *DR5*, *MtWOX5*, *MtPLT1*, *MtPLT2*, *MtPLT3*, *MtPLT4* and *TCS*, distinct gene expression signatures can be distinguished within the NM. One region is at the periphery of the nodule and includes the NVM; here, the gene activity patterns suggest that an auxin/*PLT*-directed root-like developmental program is active at each of the vascular bundle tips. A second domain is marked by high *TCS*, *MtPLT3* and *MtPLT4* activity. Cells within this second domain are centrally positioned within the NM and give rise to the central tissue. We will refer to this latter domain as the nodule central meristem (NCM). Based on our results we

Development (2015) 142, 2941-2950 doi:10.1242/dev.120774

propose that the NM is built up of two adjacent meristems: the NVM and NCM. We predict that the different levels of *MtPLT* transcripts have specific effects in the NVM and NCM.

Whereas the NVM is characterized by a high auxin response, the NCM is characterized by a higher cytokinin and a lower auxin response. The lower level of auxin signaling in the NCM is, however, sufficient to induce the expression of several auxin-responsive genes (Limpens et al., 2013; Breakspear et al., 2015; Roux et al., 2014). The expression of cytokinin signaling and synthesis genes, such as *MtCre1*, *MtARR4* (Gonzalez-Rizzo et al., 2006; Plet et al., 2011) and *MtLOG1* (Mortier et al., 2014), in the NM is in line with our observations on the cytokinin response in the NM. To what extent differences in hormone regimes are instructive in shaping the NVM and the NCM remains to be elucidated. Likewise, whether the colocalization of *TCS*, *MtPLT3* and *MtPLT4* activity in the infection zone is required for the formation of this zone remains to be determined. Despite the differences in expression patterns of *MtPLT1* and *MtPLT2* versus *MtPLT3* and *MtPLT4* in the NM, the phenotypes of *MtPLT1i,2i* and *MtPLT3i,4i* nodules were indistinguishable. This might be due either to the fact that RNAi-mediated knockdown was directed using the *ENOD12* promoter and not under an NVM-specific promoter, or to redundancy in the activity of *MtPLT* genes. Therefore, it remains unclear whether the differences in *MtPLT* activity in the NCM and NVM are instrumental for the formation of functionally distinct meristems. Comparing genes differentially regulated by either set of *MtPLT* genes and analyses of expression patterns of *MtPLT* genes in nodules of *Medicago lin* (Guan et al., 2013; Xiao et al., 2014) and *noot* (Couzigou et al., 2014) mutants, in which the development of nodule vascular bundles and of the NCM are uncoupled, might be informative in this context. Such knowledge might also uncover mechanisms underlying the communication between the NVM and NCM domains that enables proper nodule growth.

Nodules are considered to be modified lateral roots. Like lateral root primordia, nodule primordia are exclusively formed opposite the proto-xylem poles. In *Arabidopsis*, *PLT* genes are involved in lateral root formation (Hofhuis et al., 2013; Tian et al., 2014). Hence, it is conceivable that *Medicago PLT* genes are likewise involved in lateral root formation and have been co-opted by *Rhizobium* for nodule formation. Our phylogenetic analysis indicates that *PLT1/PLT2* and *PLT3/PLT7* gene pairs in *Arabidopsis* and *Medicago* formed through independent gene duplication events. This suggests that, despite the importance of the *PLT1/PLT2* gene pair for root growth in both species (Aida et al., 2004; this study), any putative co-option mechanism for a function in nodulation was independent of the gene duplication event in *Medicago*. For the *PLT3/PLT7* gene pair, in both species the *PLT3* orthologs appear to be expressed in the primary root tip, whereas *PLT7* orthologs are not (Hofhuis et al., 2013; this study; The *Medicago truncatula* Gene Expression Atlas Project). We show the importance of *MtPLT3* for nodulation, which suggests that for this gene too, co-option was independent of the duplication event. *PLT4* and *PLT5* are present in both species as a single gene. It will be interesting to investigate whether *Rhizobium* has also co-opted existing pathways involving the additional *MtPLT5* and *MtPLT7* orthologs for the initiation and outgrowth of nodule primordia, in analogy to *Arabidopsis* lateral root formation (Hofhuis et al., 2013; Vilches-Barro and Maizel, 2015).

Finally, it might be revealing to identify *Rhizobium*-controlled genes involved in regulating the expression of *MtPLT* genes to find out how root developmental programs are recruited to generate nodule primordia, form the NM and its subdomains, and maintain nodule growth. This knowledge should uncover how *Rhizobium* has co-opted and subsequently modified existing developmental pathways.

MATERIALS AND METHODS

Constructs

DNA fragments of putative promoter regions of *MtPLT* genes (1.5 kb for *MtPLT1*, 1.3 kb for *MtPLT2*, 2.7 kb for *MtPLT3* and 1.1 kb for *MtPLT4*) were generated by PCR using *Medicago* genomic DNA as a template and Phusion high-fidelity DNA polymerase (Finnzymes) and specific primers (supplementary material Table S5). Fragments were cloned into pENTR-D-TOPO (Invitrogen), verified by nucleotide sequence analysis, and recombined into the modified Gateway vector pK7GWIWG2(II)-UBQ10::DsRED-GUS-GFP (Karimi et al., 2002).

DNA of single *MtPLT* genes for RNAi constructs was generated by RT-PCR of cDNA made from *Medicago* nodule RNA using Phusion polymerase and gene-specific primers (supplementary material Table S5). These fragments were used as templates to obtain DNA fragments for double and quadruple RNAi constructs.

The PCR strategy used to obtain these latter fragments is based on the In-Fusion HD Cloning Kit user manual (Clontech Laboratories) and relies on the use of short overlaps to directionally clone multiple fragments by PCR. The strategy is outlined in supplementary material Table S6 and the primers, which map to exonic DNA, are given in supplementary material Table S5. To generate *MtPLT1-MtPLT2* and *MtPLT3-MtPLT4* DNA fragments for double RNAi constructs, the DNA fragments of single genes were diluted 1:500 and used as a template in a first PCR to introduce short overlaps. Subsequently, PCR products were diluted 1:500 and used in a second PCR to create a single amplicon (supplementary material Table S6). This final PCR fragment was cloned into pENTR-D-TOPO and recombined into the Gateway-compatible binary vector pENOD12-pK7GWIWG2(II)-UBQ10::DsRED (Limpens et al., 2004; Ivanov et al., 2012) to create the final RNAi construct.

Similarly, for the quadruple RNAi of *MtPLT* genes, the *MtPLT1-MtPLT2* and *MtPLT3-MtPLT4* PCR fragments generated above were amplified using the primer combinations shown in supplementary material Table S5 to introduce short overlaps. The fragments obtained were diluted and combined in a second PCR to create a single amplicon, which was cloned into pENTR-D-TOPO and subsequently recombined into the Gateway-compatible binary vector pENOD12-pK7GWIWG2(II)-UBQ10::DsRED or in 35S-pK7GWIWG2(II)-UBQ10::DsRED (Limpens et al., 2004; Ivanov et al., 2012).

Hairy root transformation

All constructed binary vectors were introduced into *M. truncatula* A17 through *A. rhizogenes*-mediated transformation as described (Limpens et al., 2004). Plants carrying transgenic roots were grown in perlite for 8 days for root phenotype and for 15 days in the presence of *Sinorhizobium meliloti* 2011 to induce nodules. For each experiment, at least 15 individual roots and nodules were examined. Statistical analyses on nodule numbers were conducted using the Mann-Whitney test for non-normal distributions, under the assumption that nodule formation in two groups of analyzed nodulated roots is independent and ordinal.

Expression analysis and histochemical GUS staining

Plant tissues containing promoter-GUS fusions were incubated at 37°C in 0.1 M NaH_2PO_4-Na_2HPO_4 (pH 7) buffer including 3% sucrose, 0.05 mM EDTA, 0.5 mg/ml X-gluc, 2.5 mM potassium ferrocyanide and potassium ferricyanide. Incubation time varied depending on tissues and different promoter-GUS fusions. GUS-stained roots were cleared using chloral hydrate (Mayer et al., 1991). Whole-mount images of roots were taken with an Axio Imager A1 microscope (Zeiss) supplied with Nomarski optics.

Histological analysis and microscopy

Root tips and nodules were fixed in 5% glutaraldehyde in 0.1 M phosphate buffer (pH 7.2) for 1-2 h under vacuum, then washed with 0.1 M phosphate buffer four times for 15 min each, once with water for 15 min, and

Development (2015) 142, 2941-2950 doi:10.1242/dev.120774

dehydrated for 10 min in 10%, 30%, 50%, 70%, 90% and 100% ethanol, and sequentially embedded in Technovit 7100 (Heraeus Kulzer). Sections were prepared at 5-10 µm using a microtome (RJ2035, Leica), stained either with 0.05% Toluidine Blue (Sigma) or 0.1% Ruthenium Red (Sigma), mounted in Euparal (Carl Roth), and analyzed with a Leica AU5500B microscope equipped with a DFC425c camera (Leica). At least ten GUS-stained nodules from each transformation experiment were sectioned and analyzed. Representative sections are depicted.

RNA *in situ* hybridization

The 15-day-old nodules were fixed with 4% paraformaldehyde mixed with 3% glutaraldehyde in 50 mM phosphate buffer (pH 7.4) and embedded in paraffin (Paraplast X-tra, McCormick Scientific). Nodule sections of 7 µm were prepared by RJ2035 microtome. RNA ISH was conducted according to the Affymetrix user manual for ViewRNA ISH Tissue 2-plex Assay (http://www.panomics.com/UserDocs). RNA ISH probe sets were designed and produced by Affymetrix. Each set contains 20 oligonucleotide probes, each consisting of a target-specific region and a unique sequence upon which signal amplification is built. Probe sets for *MtPLT1* covered the region 122-1163 nt (1569 nt), for *MtPLT2* the region 317-1289 nt (1632 nt), for *MtPLT3* the region 123-1150 nt (1545 nt) and for *MtPLT4* the region 586-1529 nt (2070 nt) of the full-length mRNAs.

Slides were analyzed with an AU5500B microscope equipped with a DFC425c camera (both Leica).

Acknowledgements

We thank Tom Guilfoyle for sharing *DR5*; Bruno Müller for *TCS*; and Gabino Sanchez-Perez for help with the phylogenetic analysis.

Competing interests

The authors declare no competing or financial interests.

Author contributions

H.J.F., O.K. and R.H. developed the approach; H.J.F., T.T.X., O.K. and X.W. performed experiments; H.J.F., O.K., T.T.X., B.S., T.B. and R.H. edited the manuscript prior to submission.

Funding

This work was supported by the Netherlands Organization for Scientific Research [WOTRO 86-160 to X.W.].

Supplementary material

Supplementary material available online at
http://dev.biologists.org/lookup/suppl/doi:10.1242/dev.120774/-/DC1

References

Aida, M., Beis, D., Heidstra, R., Willemsen, V., Blilou, I., Galinha, C., Nussaume, L., Noh, Y.-S., Amasino, R. and Scheres, B. (2004). The PLETHORA genes mediate patterning of the Arabidopsis root stem cell niche. *Cell* **119**, 109-120.

Blilou, I., Xu, J., Wildwater, M., Willemsen, V., Paponov, I., Friml, J., Heidstra, R., Aida, M., Palme, K. and Scheres, B. (2005). The PIN auxin efflux facilitator network controls growth and patterning in Arabidopsis roots. *Nature* **433**, 39-44.

Boutilier, K., Offringa, R., Sharma, V. K., Kieft, H., Ouellet, T., Zhang, L., Hattori, J., Liu, C.-M., van Lammeren, A. A. M., Miki, B. L. A. et al. (2002). Ectopic expression of BABY BOOM triggers a conversion from vegetative to embryonic growth. *Plant Cell* **14**, 1737-1749.

Breakspear, A., Liu, C., Roy, S., Stacey, N., Rogers, C., Trick, M., Morieri, G., Mysore, K. S., Wen, J., Oldroyd, G. E. D. et al. (2015). The root hair "Infectome" of Medicago truncatula uncovers changes in cell cycle genes and reveals a requirement for auxin signaling in rhizobial infection. *Plant Cell* **26**, 4680-4701.

Bright, L. J., Liang, Y., Mitchell, D. M. and Harris, J. M. (2005). The LATD gene of Medicago truncatula is required for both nodule and root development. *Mol. Plant Microbe Interact.* **18**, 521-532.

Cebolla, A., Vinardell, J. M., Kiss, E., Oláh, B., Roudier, F., Kondorosi, A. and Kondorosi, E. (1999). The mitotic inhibitor ccs52 is required for endoreduplication and ploidy-dependent cell enlargement in plants. *EMBO J.* **18**, 4476-4484.

Couzigou, J.-M., Mondy, S., Sahl, L., Gourion, B. and Ratet, P. (2014). To be or noot to be: evolutionary tinkering for symbiotic organ identity. *Plant Signal. Behav.* **8**, e24969.

de Billy, F., Grosjean, C., May, S., Bennett, M. and Cullimore, J. V. (2001). Expression studies on AUX1-like genes in Medicago truncatula suggest that auxin is required at two steps in early nodule development. *Mol. Plant Microbe Interact.* **14**, 267-277.

Desbrosses, G. J. and Stougaard, J. (2011). Root nodulation: a paradigm for how plant-microbe symbiosis influences host developmental pathways. *Cell Host Microbe* **10**, 348-358.

Di Laurenzio, L., Wysocka-Diller, J., Malamy, J. E., Pysh, L., Helariutta, Y., Freshour, G., Hahn, M. G., Feldmann, K. A. and Benfey, P. N. (1996). The SCARECROW gene regulates an asymmetric cell division that is essential for generating the radial organization of the Arabidopsis root. *Cell* **86**, 423-433.

Dolan, L., Janmaat, K., Willemsen, V., Linstead, P., Poethig, S., Roberts, K. and Scheres, B. (1993). Cellular organization of the Arabidopsis thaliana root. *Development* **119**, 71-84.

Frugier, F., Kosuta, S., Murray, J. D., Crespi, M. and Szczyglowski, K. (2008). Cytokinin: secret agent of symbiosis. *Trends Plant Sci.* **13**, 115-120.

Galinha, C., Hofhuis, H., Luijten, M., Willemsen, V., Blilou, I., Heidstra, R. and Scheres, B. (2007). PLETHORA proteins as dose-dependent master regulators of Arabidopsis root development. *Nature* **449**, 1053-1057.

Gonzalez-Rizzo, S., Crespi, M. and Frugier, F. (2006). The Medicago truncatula CRE1 cytokinin receptor regulates lateral root development and early symbiotic interaction with Sinorhizobium meliloti. *Plant Cell* **18**, 2680-2693.

Guan, D., Stacey, N., Liu, C., Wen, J., Mysore, K. S., Torres-Jerez, I., Vernie, T., Tadege, M., Zhou, C., Wang, Z.-y. et al. (2013). Rhizobial infection is associated with the development of peripheral vasculature in nodules of Medicago truncatula. *Plant Physiol.* **162**, 107-115.

Heidstra, R. and Sabatini, S. (2014). Plant and animal stem cells: similar yet different. *Nat. Rev. Mol. Cell Biol.* **15**, 301-312.

Herrbach, V., Remblière, C., Gough, C. and Bensmihen, S. (2014). Lateral root formation and patterning in Medicago truncatula. *J. Plant Physiol.* **171**, 301-310.

Hirsch, A. M., Larue, T. A. and Doyle, J. (1997). Is the legume nodule a modified root or stem or an organ sui generis? *Crit. Rev. Plant Sci.* **16**, 361-392.

Hofhuis, H., Laskowski, M., Du, Y., Prasad, K., Grigg, S., Pinon, V. and Scheres, B. (2013). Phyllotaxis and rhizotaxis in Arabidopsis are modified by three PLETHORA transcription factors. *Curr. Biol.* **23**, 956-962.

Horstman, A., Willemsen, V., Boutilier, K. and Heidstra, R. (2014). AINTEGUMENTA-LIKE proteins: hubs in a plethora of networks. *Trends Plant Sci.* **19**, 146-157.

Ivanov, S., Fedorova, E. E., Limpens, E., De Mita, S., Genre, A., Bonfante, P. and Bisseling, T. (2012). Rhizobium-legume symbiosis shares an exocytotic pathway required for arbuscule formation. *Proc. Natl. Acad. Sci. USA* **109**, 8316-8321.

Karimi, M., Inzé, D. and Depicker, A. (2002). GATEWAY™ vectors for Agrobacterium-mediated plant transformation. *Trends Plant Sci.* **7**, 193-195.

Limpens, E. and Bisseling, T. (2003). Signaling in symbiosis. *Curr. Opin. Plant Biol.* **6**, 343-350.

Limpens, E., Ramos, J., Franken, C., Raz, V., Compaan, B., Franssen, H., Bisseling, T. and Geurts, R. (2004). RNA interference in Agrobacterium rhizogenes-transformed roots of Arabidopsis and Medicago truncatula. *J. Exp. Bot.* **55**, 983-992.

Limpens, E., Ivanov, S., van Esse, W., Voets, G., Fedorova, E. and Bisseling, T. (2009). Medicago N2-fixing symbiosomes acquire the endocytic identity marker Rab7 but delay the acquisition of vacuolar identity. *Plant Cell* **21**, 2811-2828.

Limpens, E., Moling, S., Hooiveld, G., Pereira, P. A., Bisseling, T., Becker, J. D. and Küster, H. (2013). Cell- and tissue-specific transcriptome analyses of Medicago truncatula root nodules. *PLoS ONE* **8**, e64377.

Mähönen, A. P., ten Tusscher, K., Siligato, R., Smetana, O., Díaz-Triviño, S., Salojärvi, J., Wachsman, G., Prasad, K., Heidstra, R. and Scheres, B. (2014). PLETHORA gradient formation mechanism separates auxin responses. *Nature* **515**, 125-129.

Mathesius, U., Weinman, J. J., Rolfe, B. G. and Djordjevic, M. A. (2000). Rhizobia can induce nodules in white clover by "hijacking" mature cortical cells activated during lateral root development. *Mol. Plant Microbe Interact.* **13**, 170-182.

Mayer, U., Ruiz, R. A. T., Berleth, T., Miseéra, S. and Juürgens, G. (1991). Mutations affecting body organization in the Arabidopsis embryo. *Nature* **353**, 402-407.

Mortier, V., Wasson, A., Jaworek, P., De Keyser, A., Decroos, M., Holsters, M., Tarkowski, P., Mathesius, U. and Goormachtig, S. (2014). Role of LONELY GUY genes in indeterminate nodulation on Medicago truncatula. *New Phytol.* **202**, 582-593.

Müller, B. and Sheen, J. (2008). Cytokinin and auxin interaction in root stem-cell specification during early embryogenesis. *Nature* **453**, 1094-1097.

Nutman, P. S. (1948). Physiological studies on nodule formation. 1. The relation between nodulation and lateral root formation in red clover. *Ann. Bot.* **12**, 81-96.

Osipova, M. A., Dolgikh, E. A. and Lutova, L. A. (2011). Features of the expression of a meristem-specific WOX5 gene during nodule organogenesis in legumes. *Ontogenez* **42**, 264-275.

Osipova, M. A., Mortier, V., Demchenko, K. N., Tsyganov, V. E., Tikhonovich, I. A., Lutova, L. A., Dolgikh, E. A. and Goormachtig, S. (2012). WUSCHEL-RELATED HOMEOBOX5 gene expression and interaction of CLE peptides with components of the systemic control add two pieces to the puzzle of autoregulation of nodulation. *Plant Physiol.* **158**, 1329-1341.

Petersson, S. V., Johansson, A. I., Kowalczyk, M., Makoveychuk, A., Wang, J. Y., Moritz, T., Grebe, M., Benfey, P. N., Sandberg, G. and Ljung, K. (2009). An auxin gradient and maximum in the Arabidopsis root apex shown by high-

resolution cell-specific analysis of IAA distribution and synthesis. *Plant Cell* **21**, 1659-1668.

Plet, J., Wasson, A., Ariel, F., Le Signor, C., Baker, D., Mathesius, U., Crespi, M. and Frugier, F. (2011). MtCRE1-dependent cytokinin signaling integrates bacterial and plant cues to coordinate symbiotic nodule organogenesis in Medicago truncatula. *Plant J.* **65**, 622-633.

Prasad, K., Grigg, S. P., Barkoulas, M., Yadav, R. K., Sanchez-Perez, G. F., Pinon, V., Blilou, I., Hofhuis, H., Dhonukshe, P., Galinha, C. et al. (2011). Arabidopsis PLETHORA transcription factors control phyllotaxis. *Curr. Biol.* **21**, 1123-1128.

Roudier, F., Fedorova, E., Lebris, M., Lecomte, P., Györgyey, J., Vaubert, D., Horvath, G., Abad, P., Kondorosi, A. and Kondorosi, E. (2003). The Medicago species A2-type cyclin is auxin regulated and involved in meristem formation but dispensable for endoreduplication-associated developmental programs. *Plant Physiol.* **131**, 1091-1103.

Roux, B., Rodde, N., Jardinaud, M.-F., Timmers, T., Sauviac, L., Cottret, L., Carrère, S., Sallet, E., Courcelle, E., Moreau, S. et al. (2014). An integrated analysis of plant and bacterial gene expression in symbiotic root nodules using laser-capture microdissection coupled to RNA sequencing. *Plant J.* **77**, 817-837.

Sabatini, S., Beis, D., Wolkenfelt, H., Murfett, J., Guilfoyle, T., Malamy, J., Benfey, P., Leyser, O., Bechtold, N., Weisbeek, P. et al. (1999). An auxin-dependent distal organizer of pattern and polarity in the Arabidopsis root. *Cell* **99**, 463-472.

Sabatini, S., Heidstra, R., Wildwater, M. and Scheres, B. (2003). SCARECROW is involved in positioning the stem cell niche in the Arabidopsis root meristem. *Genes Dev.* **17**, 354-358.

Sarkar, A. K., Luijten, M., Miyashima, S., Lenhard, M., Hashimoto, T., Nakajima, K., Scheres, B., Heidstra, R. and Laux, T. (2007). Conserved factors regulate signalling in Arabidopsis thaliana shoot and root stem cell organizers. *Nature* **446**, 811-814.

Stougaard, J. (2001). Genetics and genomics of root symbiosis. *Curr. Opin. Plant Biol.* **4**, 328-335.

Tamura, K., Peterson, D., Peterson, N., Stecher, G., Nei, M. and Kumar, S. (2011). MEGA5: Molecular evolutionary genetics analysis using maximum likelihood, evolutionary distance, and maximum parsimony methods. *Mol. Biol. Evol.* **28**, 2731-2739.

Tian, H., Jia, Y., Niu, T., Yu, Q. and Ding, Z. (2014). The key players of the primary root growth and development also function in lateral roots in Arabidopsis. *Plant Cell Rep.* **33**, 745-753.

Timmers, A. C. J., Auriac, M. C. and Truchet, G. (1999). Refined analysis of early symbiotic steps of the Rhizobium-Medicago interaction in relationship with microtubular cytoskeleton rearrangements. *Development* **126**, 3617-3628.

van den Berg, C., Willemsen, V., Hendriks, G., Weisbeek, P. and Scheres, B. (1997). Short-range control of cell differentiation in the Arabidopsis root meristem. *Nature* **390**, 287-289.

Vilches-Barro, A. and Maizel, A. (2015). Talking through walls: mechanisms of lateral root emergence in Arabidopsis thaliana. *Curr. Opin. Plant Biol.* **23**, 31-38.

Xiao, T. T., Schilderink, S., Moling, S., Deinum, E. E., Kondorosi, E., Franssen, H., Kulikova, O., Niebel, A. and Bisseling, T. (2014). Fate map of Medicago truncatula root nodules. *Development* **141**, 3517-3528.

Zürcher, E., Tavor-Deslex, D., Lituiev, D., Enkerli, K., Tarr, P. T. and Muller, B. (2013). A robust and sensitive synthetic sensor to monitor the transcriptional output of the cytokinin signaling network in planta. *Plant Physiol.* **161**, 1066-1075.

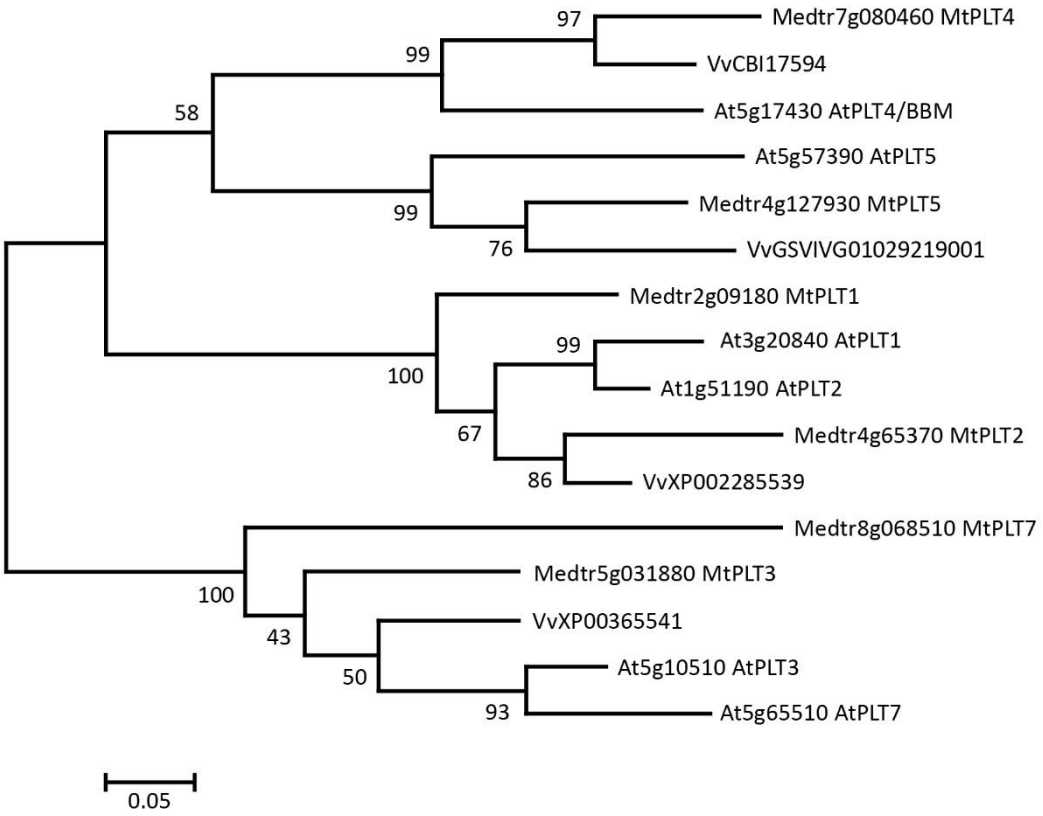

Fig. S1. Orthology between Arabidopsis and Medicago *PLT* genes.
Maximum likelihood phylogenetic tree of PLETHORA proteins from Arabidopsis, Medicago and *Vitis venifera* (as outgroup). The Arabidopsis protein names are according to Prasad et al 2011 , resolving the tree into four clades, the PLT1/2, PLT3/7, PLT4 and PLT5 clades respectively. The Medicago protein sequences were obtained after reciprocal BLAST of Arabidopsis protein sequences through TBLASTN on Mt4.0 v1CDS (http://blast.jcvi.org/er-blast/index.cgi?project=mtbe) followed by BLASTX against the Arabidopsis protein database of the nucleotide sequences of the retrieved Medicago proteins. The Vitis proteins were retrieved by BLASTP of Arabidopsis proteins. The Vitis genome contains one gene copy for each of the four clades. The midpoint rooted tree was constructed with MEGA version 5.1 (Tamura et al., 2011), using default parameters (bootstrap values of 500 replicates).

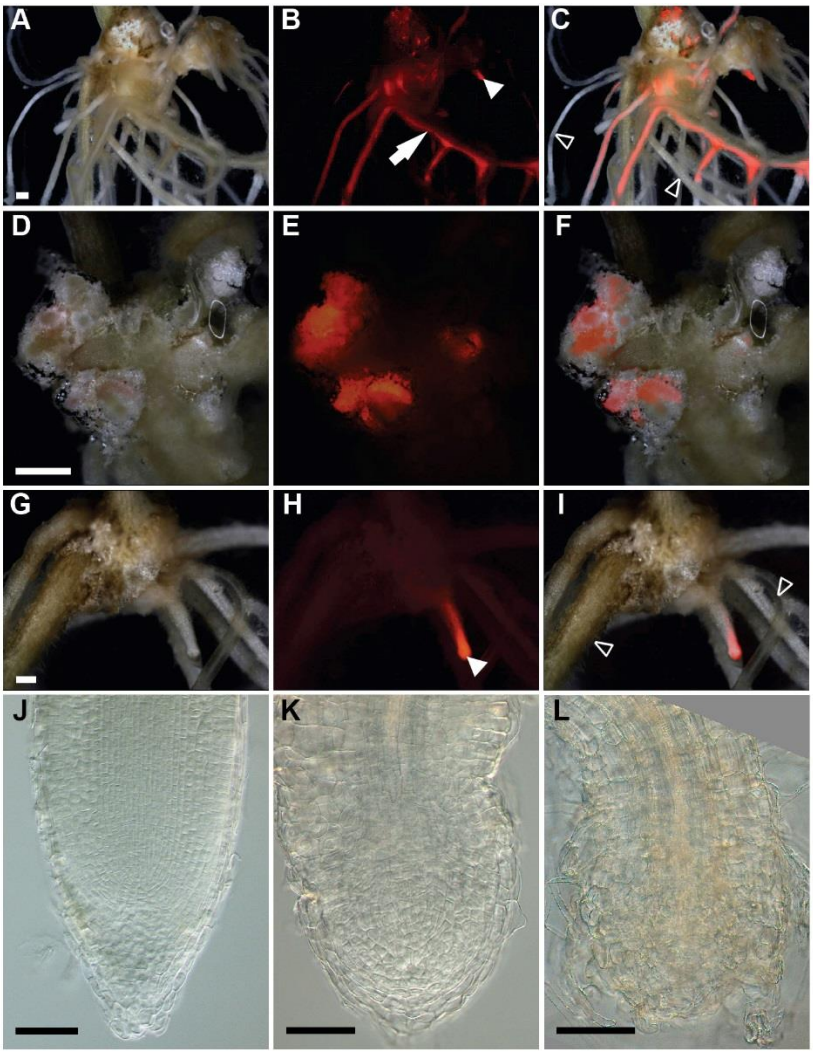

Fig. S2. Transgenic hairy root formation requires *MtPLT1-4* gene expression
(A-I) Vector control transgenic calli readily generate hairy roots (A-C, arrow, arrowhead), in contrast to *35S::MtPLTi* transgenic calli (D-I). (J-L) Occasionally from some *35S::MtPLTi* calli short transgenic roots appear (H; arrowhead), compared to long roots formed on vector control transgenic calli (B, arrow). When compared to vector control roots (J), the meristem of these short roots is severely affected or absent soon after emergence (K, L; note the presence of root hairs as a marker for differentiation). (M) Average number of short and long roots formed on transgenic calli of *35S::MtPLT1i,2i*, *35S::MtPLT3i,4i*, *35S::MtPLTi* and empty vector control transgenic roots, shows that *35S::MtPLTi* leads to a strong reduction in roots formed from transgenic calli.
(A, D, G) Bright field; (B, E, H) dsRed filter; (C, F, I) overlay. (J-L) Bright field with Nomarski objectives.

Bars 240µm (A-I) and 75µm (J-L).

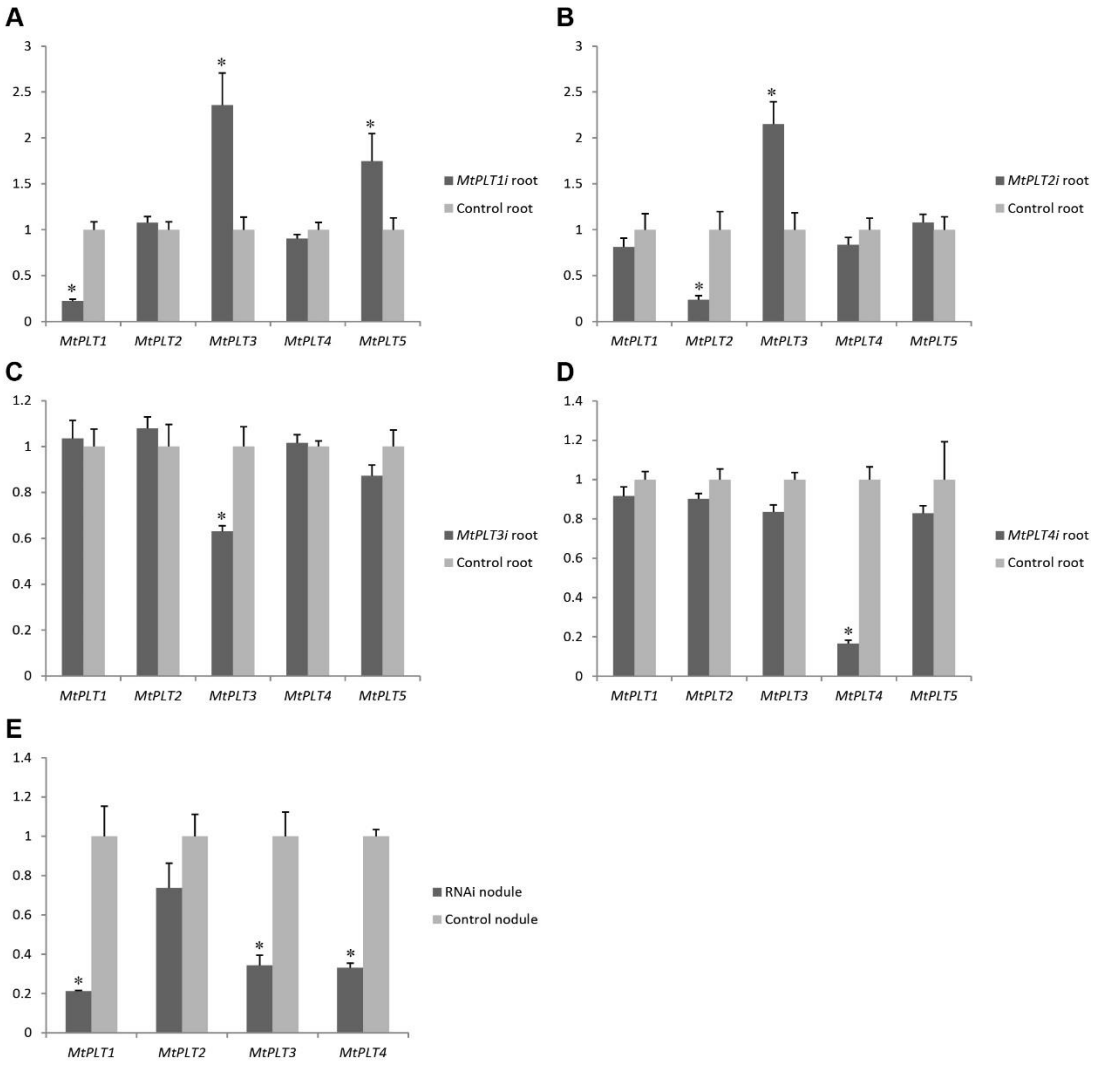

Fig. S3. *MtPLT* expression levels in single *35S::MtPLT* RNAi root and nodules.
(A-E) Relative *MtPLT* expression in single *35S::MtPLT* RNAi roots (A-D, gray bar) and 15 d old nodules (E, gray bar) compared to their expression in control roots and nodules (black bar), respectively. Relative expression levels were determined by qPCR and normalized to 1 in control plants for each *MtPLT* gene using *MtACTIN-2*. Shown graphs are the means ± s.e.m. of two biological repeats. Significance of expression reduction of tested *MtPLT* gene in RNAi versus expression of this gene in control samples is indicated by * as $P<0.05$ in Student t test.

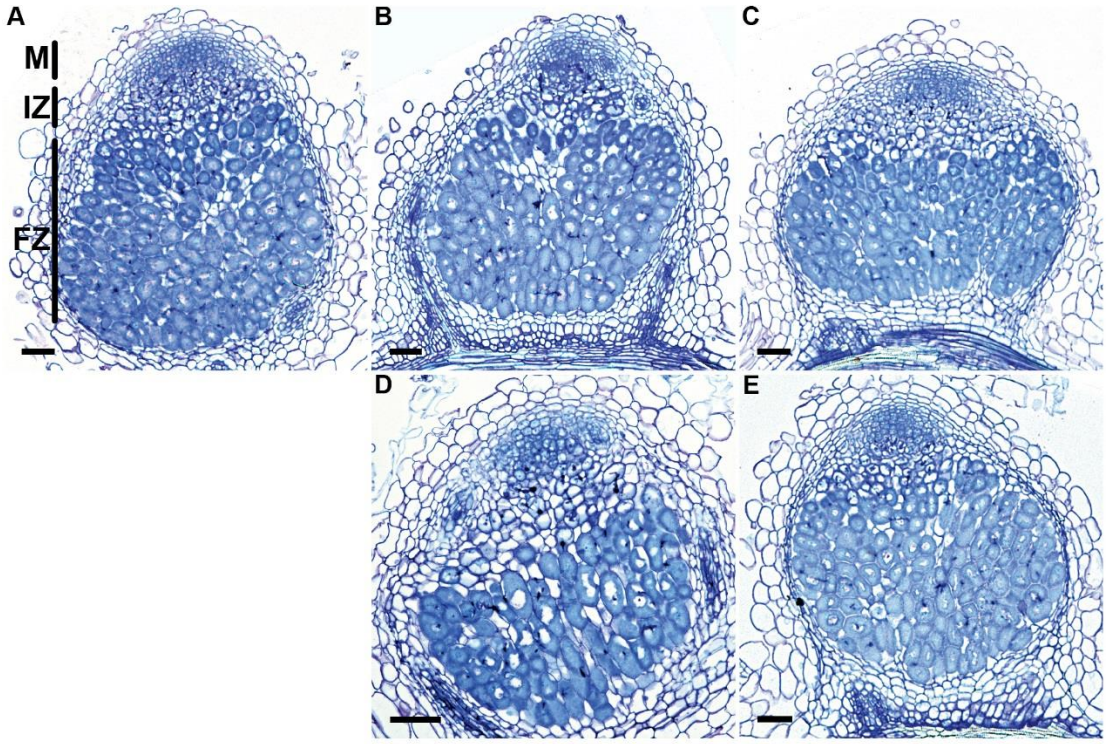

Fig. S4. Longitudinal sections of representative single *MtPLT* RNAi nodules.
(A) Median section through a control nodule. (B-E) representative median section through *35S::MtPLT1i* (B), *35S::MtPLT2i* (C), *35S::MtPLT3i* (D) and *35S::MtPLT4i* (E) nodule. All nodules were sampled 15 d after inoculation. For statistics on cell layers per zone see Table S3. M, meristem; IZ, infection zone; FZ, fixation zone.

Bars 75μm.

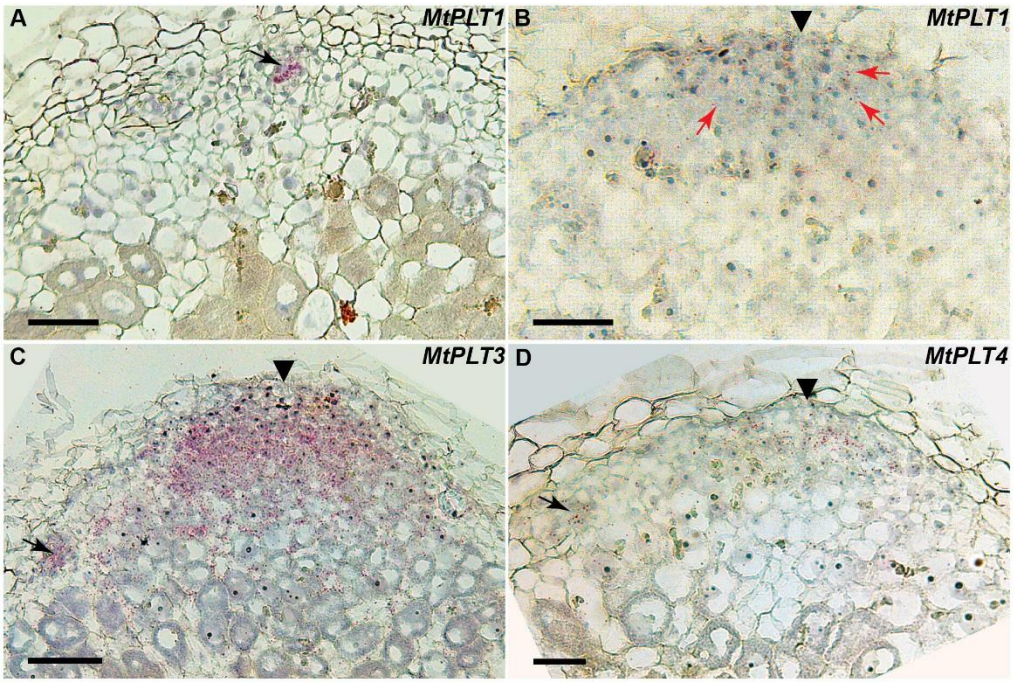

Fig. S5. RNA *In situ* hybrization of *MtPLT1*, *MtPLT3* and *MtPLT4* in nodules.
To validate the *pMtPLT::GUS* patterns, we conducted ISH on sections of 15day old nodules with gene specific probes of (A, B) *MtPLT1*, (C) *MtPLT3* and (D) *MtPLT4* visualized as pink grains. (A, B) Note the high expression level of *MtPLT1* in NVM (A, arrow) and the very low level in the NCM (B, arrowhead). (C) *MtPLT3* expression is in the NM and in the infection zone, while (D) *MtPLT4* expression is restricted to NM. The *MtPLT2* ISH expression pattern described (Roux et al., 2014) is in agreement with the *pMtPLT2::GUS* expression pattern (Fig. 6 G-I) and for *MtPLT1,3,4* genes the ISH pattern is similar to the *pMtPLT1,3,4::GUS* pattern (Fig. 6 G-L), respectively. This indicates that the *pMtPLT::GUS* patterns are reflecting *MtPLT* transcripts. Arrows point to NVM, arrowheads to NCM. Red arrows in B point to individual grains indicating the low expression of *MtPLT1* in the NCM.

Bars 75µm.

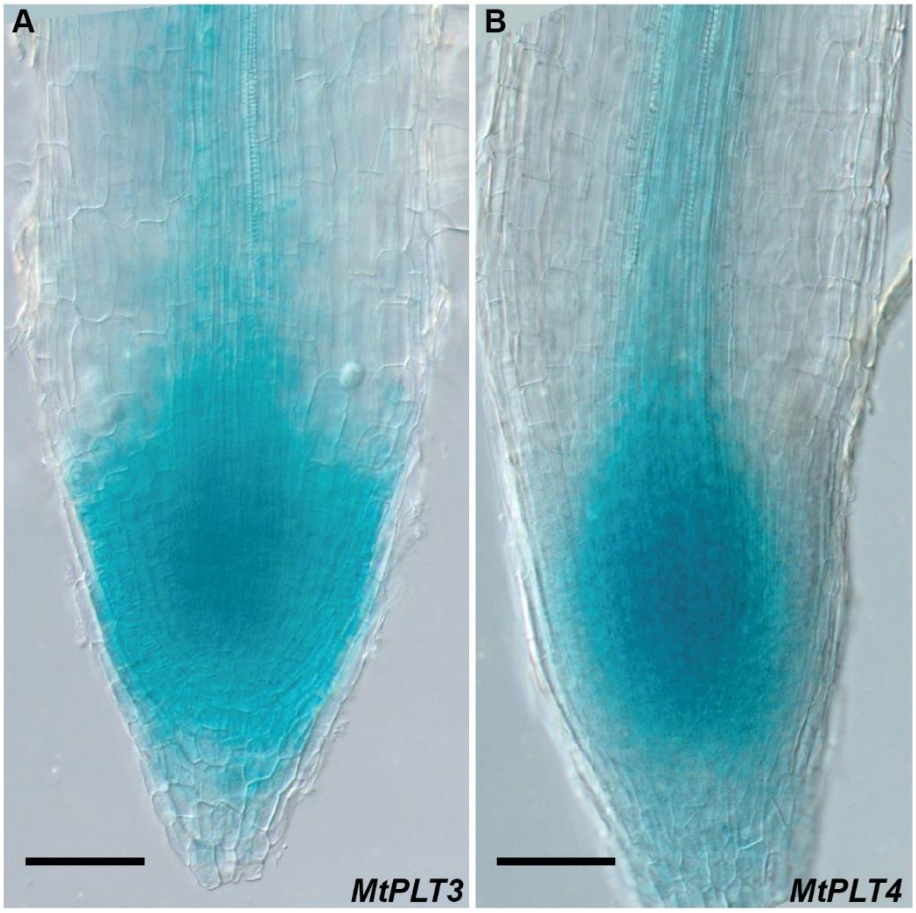

Fig. S6. *MtPLT3::GUS* and *MtPLT4::GUS* expression patterns in the root.
(A) *MtPLT3::GUS* and (B) *MtPLT4::GUS* expression patterns extend into the root vascular tissue.

Bars 75µm.

Table S1. Root formation and growth upon *35S::MtPLT* RNAi transformation

SR, short roots (<3 cm); LR, long roots (>3 cm).

transgene	Calli	Roots	SR	LR	Roots/callus
35S::EV	18	62	4	58	3.5
35S::MtPLT1i,2i	20	22	13	9	~1
35S::MtPLT3i,4i	27	78	12	66	~3
35S::MtPLTi	16	4	4	0	0.25
pENOD12::EV	16	41	2	39	2.5
pENOD12::MtPLTi	16	32	1	31	2

Table S2. Nodule formation on *35S::MtPLT* RNAi transgenic roots.

Number of nodules/root in two independent experiments involving at least 15 roots per experiment. Data was collected 15 days after inoculation. EV is empty vector.

	Number of analysed roots	Nodules/root
35S::EV	70	3.2±0.2
35S::MtPLT1i	46	3.1±0.1
35S::MtPLT2i	32	3.3±0.2
35S::MtPLT3i	42	3.1±0.4
35S::MtPLT4i	49	3.4±0.2

Table S3. Quantification of nodule histology upon single *35S::MtPLT* RNAi

Analyses of 20 control nodules shows that the meristem consists of 4-6 cell-layers and the central tissue of 16-19 cell layers distributed over 6-7 cell-layers in the infection zone and 10-12 cell layers in the fixation zone. Compared to control nodules, all zones of single *35S::MtPLT* RNAi nodules consist of a number of cell layers that is within the variation observed in the control. Data was collected in two biological replicas and 15 days after inoculation.

	Meristem	Infection zone	Fixation zone	Nodule number
control	4-6	6-7	10-12	20
MtPLT1i	4-6	6-8	10-14	19
MtPLT2i	4-7	5-7	9-10	17
MtPLT3i	4-5	6-8	8-10	20
MtPLT4i	4-7	7-9	8-12	17

Table S4. Nodule formation on *ENOD12::MtPLT* RNAi transgenic hairy roots in three independent experiments

C represents nodules formed on control transgenic hairy roots generated using the empty vector only expressing the DsRED selection marker. N is the average number of nodules per root (18 roots per construct per experiment). The percentage of reduced number of nodules (%) on *MtPLT* RNAi roots is significant at P< 0.05 for *MtPLT1i,2i* and *MtPLT3i,4i* (Mann Whitney test) or at P<0.01 for *MtPLTi* (Mann Whitney test)

C (N)	*MtPLT1i,2i* (N)	%	*MtPLT3i,4i* (N)	%	*MtPLTi* (N)	%
5.8	3.1	47	3	49	1	83
6.2	3.0	52	3.3	47	1.1	83
6.0	3.1	49	2.9	52	1.5	75

Table S5. Primers used in this study

promoters	
MtpPLT1F	caccgacttgacggtgaaggtt
MtpPLT1R	gcacaacctgcatctaaaaagtttact
MtpPLT2F	caccatccaaacacacccttagtc
MtpPLT2R	gagggaatgaaagccagttattgttc
MtpPLT4F	cacctctcaaatagaatttacctccaac
MtpPLT4R	gaaagaaaaaaaaagacaaagagagatcgg
MtpPLT3F	caccttgcactcccctcctctcaaag
MtpPLT3R	caaagtctttgaacagaaacaacgg
MtpWOX5F	cacccaaccaagccttatcatagtat
MtpWOX5R	gctctcttccatatttcaattctaga
single *MtPLTi*	
MtPLT2F	cacctgaacacacacaacagcaatgaagttcc
MtPLT2R	gaagttctttgtccaaatgtctctg
MtPLT 1F	caccccttgatgaatagtagtcacaactc
MtPLT 1R	tcttgttacaccacgatatattgatg
MtPLT 4F	caccatcatcatcaacaacacttccc
MtPLT 4R	cctttaatctcactctcacc
MtPLT 3F	caccagcttcctcttcagttg
MtPLT 3R	cactgctactaccaacttc
MtPLT 3R2	cacccactgctactaccaacttc
double *MtPLTi*	
MtPLT 1com2R	gttgtgtgtgttcagccttgttacaccacg
MtPLT 2com1F	cgtggtgtaacaaggctgaacacacacaacag
MtPLT 4com3R	caactgaagagcatcatcaacaac
MtPLT 3com4F	gttgttgatgatgctcttcagttg
Quadruple *MtPLTi*	
12-43F	gggaagtgttgttgagaatagtagtcacaactc
43-12R	gagttgtgactactattctcaacaacacttccc
MtPLT 3R2	cacccactgctactaccaacttc
qPCR primers	
qMtPLT4F	tcacgaggtgcatccatttaccga
qMtPLT4R	acatcatatgcctctgctgcctct
qMtPLT1F2	ggaacttttggtaccgaggaa
qMtPLT1R2	tttgcagcacctcctcctat
qMtPLT2R	gcaatggttgaggttgttca
qMtPLT2F2	tcgagaaaacgcgaagaaat
qMtPLT3R	gttgctgctgctgctgttag
qMtPLT3F	tgacgtggaagcgataatga
qMtACT2F	cagatgtggatctccaagggtga
qMtACT2R	tgactgaaatatggcacaagactgaga
qMtPLT5F	cagtgataatccccacaatgc
qMtPLT5R	aagaaaatattggcgttgcg
qMtPLT7F	agaggcatacgaccttgcag
qMtPLT7R	ggaaggttttaagcgttttgc

Table S6. Strategy to obtain *MtPLT* DNA fragments for cloning into RNAi vectors.

Input fragment	First PCR primers	Second PCR primers	Final fragment
MtPLT1	MtPLT1F+Mt PLT1com2R	MtPLT1F+MtPLT2R	MtPLT1-MtPLT2
MtPLT2	MtPLT2com1F+MtPLT2R		
MtPLT3	MtPLT3com4F+MtPLT3R	MtPLT4F+ MtPLT3R	MtPLT3-MtPLT4
MtPLT4	plt4F+plt4com3R		
MtPLT1-MtPLT2	12-34F+MtPLT2R	MtPLT3R2+ MtPLT2R	MtPLT3-MtPLT4-MtPLT1-MtPLT2
MtPLT4-MtPLT3	MtPLT3R2+34-12R		